FERMILAB-CONF-20-306-ND

ABCD-ABCD

Baby MIND detector first physics run

A. Ajmi[1] ,Y. Asada[2], P. Benoit[3], A. Blondel[4], M. Bogomilov[5], A. Bonnemaison[6], A. Bross[7], F. Cadoux[4], S. Cao[8], A. Cervera[9], N. Chikuma[10], R. Cornat[6], L. Domine[6], O. Drapier[6], A. Dudarev[3], A. Eguchi[10], T. Ekelöf[11], Y. Favre[4], S. Fedotov[12], O. Ferreira[6], F. Gastaldi[6], M. Gonin[6], Y. Hayato[13], A. Hiramoto[1], T. Honjo[14], A.K. Ichikawa[1], J. Imber[6], M. Khabibullin[12], A. Khotyantsev[12], T. Kikawa[1], K. Kin[14],T. Kobata[14] ,T. Kobayashi[8], A. Kostin[12], Y. Kudenko[12], N. Kukita[14], S. Kuribayashi[1], M. Louzir[6] G. Mitev[15], K. Matsushita[1], A. Mefodiev[12], A. Minamino[2], F. Magniette[6], O. Mineev[12], T. Mueller[6], T. Nakaya[1], M. Nessi[3], L. Nicola[4], K. Nishiziki[14], E. Noah[4], J. Nugent[16], T.Odagawa[1], K. Okamoto[2], H. Pais Da Silva[3], S. Parsa [4 † ¶ *], G. Pintaudi[2], B. Quilain [10], M. Rayner[3], G. Rolando[3], C. Ruggles[16] F. Sanchez[4], Y. Seiya[14], F.J.P. Soler[16], S. Suvorov[12], S.Takayasu[14], S. Tanaka[14], H. Ten Kate[3], N. Teshima[14], N. Tran[17], R. Tsenov[5], G. Vankova-Kirilova[5], L. Vignoli[6], O. Volcy[6], K. Yamamoto[14], K. Yasutome[1], N. Yershov[12] and M. Yokoyama[10].

[1] *Kyoto University, Kyoto, Japan.*
[2] *Yokohama National University, Yokohama, Japan.*
[3] *European Organization for Nuclear Research, CERN, Geneva, Switzerland.*
[4] *University of Geneva, Section de Physique, DPNC, Geneva, Switzerland.*
[5] *University of Sofia, Department of Physics, Sofia, Bulgaria.*
[6] *Ecole Polytechnique, IN2P3-CNRS, Laboratoire Leprince-Ringuet, Palaiseau, France*
[7] *Fermi National Accelerator Laboratory, Batavia, Illinois, USA.*
[8] *High Energy Accelerator Research Organization (KEK), Tsukuba, Ibaraki, Japan*
[9] *IFIC (CSIC & University of Valencia), Valencia, Spain.*
[10] *University of Tokyo, Tokyo, Japan.*
[11] *University of Uppsala, Uppsala, Sweden.*
[12] *Institute of Nuclear Research, Russian Academy of Sciences, Moscow, Russia.*
[13] *University of Tokyo, Institute for Cosmic Ray Research, Kamioka Observatory, Kamioka, Japan*
[14] *Osaka City University, Department of Physics, Osaka, Japan*
[15] *Academy of Sciences, Sofia, Bulgaria*
[16] *University of Glasgow, School of Physics and Astronomy, Glasgow, UK.*
[17] *IFRISE, Quy Nhon, Vietnam.*

[†]saba.parsa@unige.ch

Abstract

Baby MIND is a Magnetized Iron Neutrino Detector, serving as a downstream magnetized muon range detector for WAGASCI on the T2K beam line in Japan. The first physics run of Baby MIND together with other WAGASCI sub-detectors took place in the period from November 2019 to February 2020 (T2K run10), where a total of 4.8×10^{20} Protons on target (POT) was delivered. Preliminary results showing Baby MIND data quality, detector performance and examples of neutrino interactions on iron during the first physics run are presented.

Presented at

NuPhys2019: Prospects in Neutrino Physics
Cavendish Conference Centre, London, 16–18 December 2019

[¶]Speaker
[*]On behalf of WAGASCI - Baby MIND collaboration

1 Introduction

Baby MIND [1] is the downstream muon range detector (MRD) of WAGASCI, located on the B2 floor of the T2K near detector complex, at a distance of 280 m downstream from the T2K beam target. The configuration of all components of WAGASCI is shown in Figure 1, including two WAGASCI target modules [WG], made of water and plastic, the Proton module [PM], made of plastic, two Wall MRDs [WMRD], made of iron and plastic and the Baby MIND detector. Detailed information about WAGASCI sub-detectors can be found in [2].

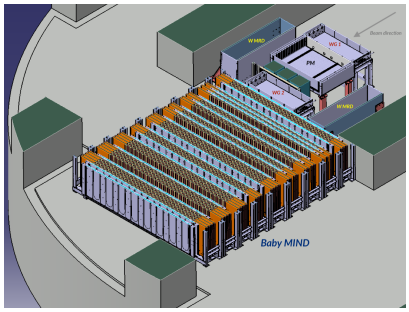

Figure 1: Layout of WAGASCI sub-detectors (cross-sectional view).

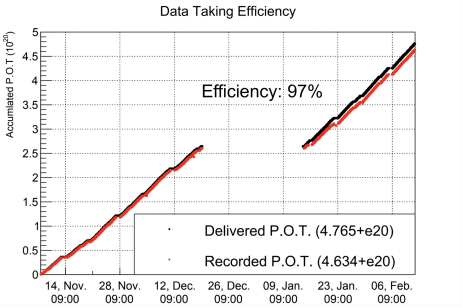

Figure 2: Baby MIND Data collection efficiency during Nov-Dec 2019.

While the main purpose of WAGASCI is to measure cross sections of charged current neutrino and antineutrino interactions on water and plastic, separate measurements can be obtained from the charged current neutrino and antineutrino interactions on iron in Baby MIND. With 33 Magnet modules made of iron, each weighing 2 tonnes, the expected number of neutrino interactions on iron in Baby MIND is far more significant than the WAGASCI target modules, which makes Baby MIND a suitable candidate for beam monitoring. The sensitive layers of the Baby MIND detector consist of 18 scintillating modules, which are interleaved with magnet modules in an irregular pattern. Despite the low resolution of Baby MIND for tracking vertex activity, due to significant non-sensitive material in the particle's path, charged current neutrino interactions on iron with a muon traversing three or more scintillating modules can be reconstructed. A summary of Baby MIND's first physics run, the detector response and event pre-selection strategy are discussed in the following sections.

2 Data collection efficiency during the first physics run

The first physics run for WAGASCI-Baby MIND in ν_μ beam mode took place between November 2019 and February 2020, coinciding with efforts to increase the T2K beam power, which eventually reached a record maximum power of 522.6 kW. During this period (T2K run 10) a total of 4.8×10^{20} Protons on target (POT) was delivered. Baby MIND succeeded in collecting the data in this period with 97 % data collection efficiency (Figure 2), thanks to the stability of all detector systems including the magnet system, the electronics, the synchronization unit, the DAQ system and the efforts of the local operation team.

3 Detector response

The detector performance studies were carried out by selecting sand muons, which are the results of neutrino interactions in the material upstream of Baby MIND including other WAGASCI sub-detector. The requirement for having at least ten active modules in Baby MIND with low hit multiplicity aims to select clean high energy muons as highly penetrating Minimum Ionizing Particles (MIP).

3.1 Readout and Calibration

The Baby MIND readout scheme [3] consists of 3996 channels instrumented by Hamamatsu photo-sensors (Multi Pixel Photon Counter - MPPC) of type S12571-025 and 28 channels by type S13081-

050CS. The readout electronics are based on the CITIROC chip. The MPPC input signal gets split in two paths, High Gain pre-amp (HG) and Low Gain pre-amp (LG), each with their own slow shapers and peak detection circuitry. The Time over Threshold (ToT) provides an additional measure of the signal strength. The HG analogue amplitude is calibrated by extracting the MPPC gain [ADC/p.e] from the dark count finger plot shown in Figures 3 and 4. HG is the most sensitive charge readout and has a range up to 100 p.e. The LG analogue amplitude is linearly proportional to HG amplitude before its saturation and has a larger range of up to 1000 p.e. Both of these analogue signal paths have a dead time of 10 μs due to multiplexing and digitization which follows a tunable hold period designated for sampling the amplitudes. For this data run, the hold duration was set to 10 μs to cover all of the eight bunches of a T2K spill. During a hold period only one value of HG and LG is registered per channel if above threshold. On the other hand, the digital signal path of ToT experiences no dead time but has a lower resolution. The calibration of ToT is achieved by fitting with respect to HG and LG. Finally the hit Light Yield (LY) is reconstructed by merging the information from the three signal paths.

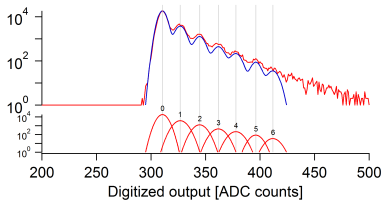

Figure 3: MPPC finger plot. Peaks represent 1, 2, 3, ... photo electrons respectively.

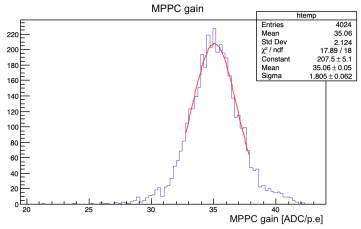

Figure 4: Distribution of MPPCs gain value [ADC/p.e].

3.2 Light yield of scintillating bars

Each of the 18 scintillating modules contains 95 horizontal bars of $2900 \times 30 \times 7.5$ mm^3 and 16 vertical bars of $1950 \times 210 \times 7.5$ mm^3. The horizontal bars each has a straight wavelength shifting (WLS) fiber whose ends are read out from two sides, while the wider vertical bars each has a U shaped WLS fiber whose ends are both read out from the top. Figure 5 shows the distribution of the mean LY, summed over both readout ends, for all horizontal (left) and vertical bars (right).

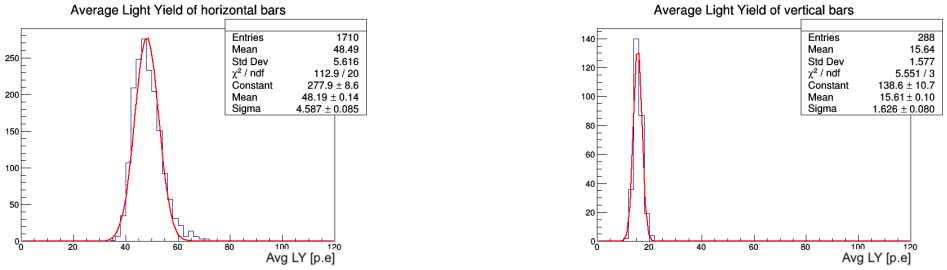

Figure 5: Distribution of the average LY summed over both ends for horizontal (left) and vertical bars (right).

3.3 Timing

The internal 400 MHz clock of the Baby MIND electronics provides hit times in units of 2.5 ns. With this sampling frequency the bunch structure of T2K beam can be clearly seen in Figure 6. The bunches are 580 ns apart and have a sigma of 25 ns each. The hit time information is primarily used to group hits and pre-select events which occur in one bunch. In order to extract high accuracy timing information such as track directionality from the time of flight, some corrections need to be applied, namely the delays induced by WLS fiber and electronics time walk. Both studies have been carried out using the sand muons sample. The effective signal propagation velocity in WLS fiber of the horizontal bars was measured to be 154.72 ± 2.12 mm/ns (Figure 7) and the time walk was

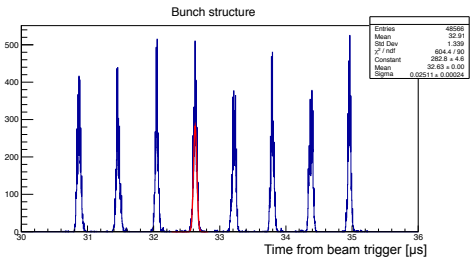

Figure 6: T2K bunch structure obtained from hit time distribution in Baby MIND.

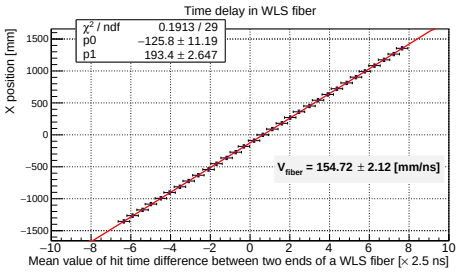

Figure 7: Velocity of propagation of light in WLS fiber.

parametrized by a double exponential function as seen in Figure 8. After these time corrections, the time of flight for through-going sand muons was investigated. In Figure 9, each point represents the module z position vs the mean value of the hit time distribution in the module relative to the hit time of the last module. Note that the angle and curvature of the tracks have not been corrected for. Based on this result, the direction of particles which have a track length of 1 m or larger can be determined with the timing capabilities of Baby MIND.

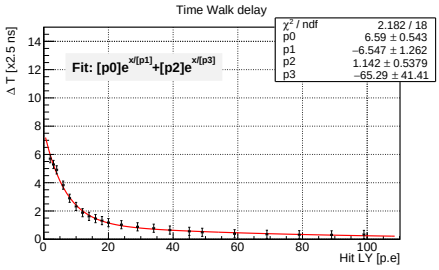

Figure 8: Time walk fit

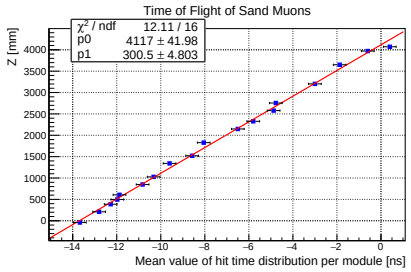

Figure 9: Time of flight of through-going sand muons.

4 Event pre-selection

The event pre-selection scheme can be described as follows. A pre-selected event is composed of two time separated objects (groups of hits) for side view (Y-Z) and top view (X-Z). Each view contains all the hits within ±50 ns. The pre-selected events are categorized based on simple topology criteria as described in Table 1. The sand muons have been chosen to study the event rate stability over all data runs in the period of December 2019. The run statistics are summarized in Table 2. The average occurrence rate of sand muons was found to be 0.92 ± 0.07 events per 10^{15} POT in December data runs.

Table 1: Event pre-selection categories.

Categories	Description	Criteria
Pre type 0	Short tracks	N active layers < 3 (at least in one view)
Pre type 1	Clean single tracks	N active layers ≥ 3 (both views) &&
		Cluster multiplicity per layer ≤ 2 &&
		Cluster pos spread per layer ≤ 5 cm
Pre type 2	Other single tracks	N active layers ≥ 3 (both views) &&
		Cluster multiplicity per layer ≤ 4 &&
		Cluster pos spread per layer ≤ 15 cm
Pre type 3	Multi tracks or pile up	all others events
	Sand Muons	(Pre type 1 $\|\|$ Pre type 2)&&
		N active layers ≥ 10 &&
		First layer is active

Table 2: Summary of pre-selected events in December runs.

Date	N Spills	Pre type 0	Pre type 1	Pre type 2	Pre type 3	Sand Muons	SM Rate [/10^{15} POT]
1-Dec	33248	32664	21985	18329	34676	8120	0.93 ±0.06
2-Dec	30295	30490	21044	16620	31844	7531	0.94 ±0.07
3-Dec	21697	21626	14830	11730	22387	5376	0.94 ±0.08
4-Dec	30384	30250	20412	16301	31336	7229	0.90 ±0.07
5-Dec	26089	25783	17464	13991	26813	6446	0.94 ±0.07
6-Dec	36417	36541	24826	20291	38937	9004	0.94 ±0.06
7-Dec	33581	32707	21761	18735	35138	8115	0.92 ±0.06
8-Dec	27831	26853	17897	15190	28457	6583	0.90 ±0.07
9-Dec	29015	28882	19090	16127	30770	7139	0.93 ±0.07
10-Dec	22336	22016	15104	12077	22914	5313	0.90 ±0.08
12-Dec	21204	20865	14249	11189	21835	5113	0.92 ±0.08
13-Dec	30605	30172	20059	16810	31922	7463	0.93 ±0.07
14-Dec	31613	31780	21245	17428	33365	7683	0.92 ±0.06
15-Dec	22984	22466	15137	12652	23831	5598	0.92 ±0.08
16-Dec	45086	43748	29243	24129	45381	10711	0.90 ±0.05
17-Dec	26569	26274	18096	13997	27297	6455	0.92 ±0.07

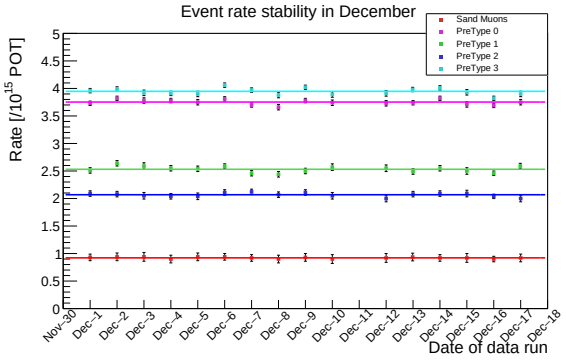

Figure 10: Pre-selected event rate in December data runs.

5 Neutrino interactions on iron

At an off-axis angle of 1.6 ° from the T2K beam direction, Baby MIND receives neutrinos with slightly higher energies than ND280 (Figure 11). The T2K ν_μ and $\overline{\nu}_\mu$ beams have a small fraction of wrong sign background (Figure 12), which can generate a muon of opposite charge in case of a charge current interaction. Baby MIND can be used to monitor the fraction of the wrong sign background with a high charge ID efficiency. Figure 13 shows such candidate events from the data. The tracks are bent in the 1.5 T magnetic field of the Baby MIND magnet modules [4].

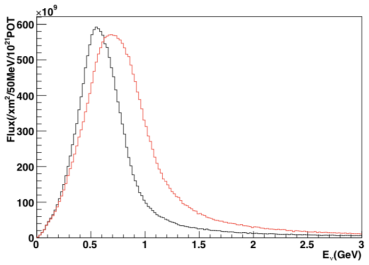

Figure 11: Neutrino Energy spectru, at Baby MIND position (red, 1.6 ° off-axis) and at ND280 position (black, 2.5 °)

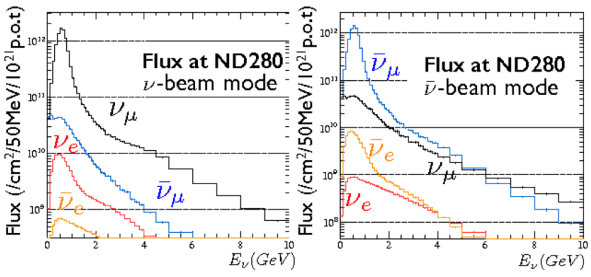

Figure 12: T2K beam contamination with other neutrino types.

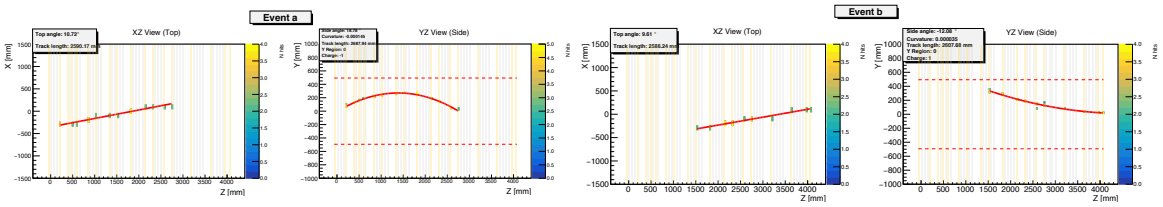

Figure 13: Top view and side view of a ν_μ-CC-QE candidate with a μ^- bending downwards in the central magnet region (left), same for a $\overline{\nu}_\mu$-CC-QE candidate with a μ^+ bending upwards (right).

However, Baby MIND observes many neutrino interactions that are not as clean and easy to reconstruct. Monte Carlo (MC) studies with neutrino flux and energies expected at the location of Baby MIND, can reveal the expected contributions of different ν_μ interaction modes on iron, which is summarized in Table 3. Examples of events with multi track or shower like topologies are presented in Figure 14.

Table 3: Contributions of different ν_μ interaction modes on iron (from Monte Carlo).

Interaction mode	CC-QE	CC-1π	CC-nπ	NC
%	37.6	21	15.5	26

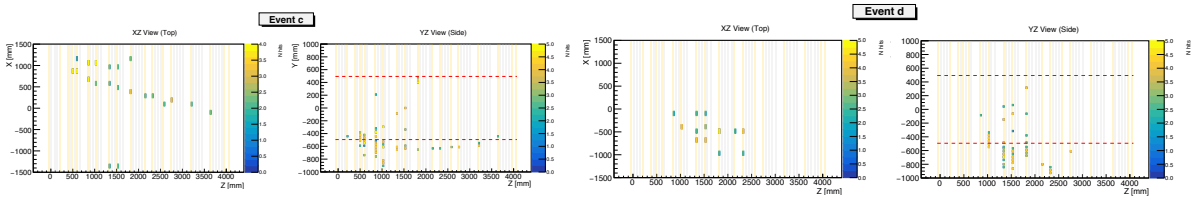

Figure 14: Top view and side view of two events with multi track and shower like topologies.

6 Summary

The first physics run of Baby MIND together with other WAGASCI subdetectors has been a successful data taking campaign with 97 % data collection efficiency. The detector performance studies such as light yield, timing and event rate stability studies have been reported and examples of neutrino interactions on iron have been presented. Prospects for the use of Baby MIND as a magnetized beam monitor for the T2K beam, with the capability of measuring the wrong sign component of the (anti)neutrino beam is under investigation.

Acknowledgements This project has received funding from the European Union's Horizon 2020 Research and Innovation programme under grant agreement No. 654168.

References

[1] S. Parsa, "Novel Design features of the Baby MIND detector for T59-WAGASCI experiment", PoS NuFact2017 (2017) 152.

[2] E. Noah *et al.*, "The WAGASCI experiment at J-PARC to measure neutrino cross-sections on water", PoS EPS-HEP2015 (2015) 292.

[3] E. Noah *et al.*, "Baby MIND Readout Electronics Architecture for Accelerator Neutrino Particle Physics Detectors Employing Silicon Photomultipliers", JPS Conf. Proc. 27, 011011 (2019)

[4] G. Rolando *et al.*, "New and Optimized Magnetization Scheme for the Baby Magnetized Iron Neutrino Detector at J-PARC", IEEE Transactions on Magnetics, May 2017, Volume 53, Issue 5.